



Generating and Focusing the Ultrasound Waves Using Elastomer-based Capacitive Micro-Speakers

M. Soosani^a, M. Fathalilou^{*a}, G. Rezazadeh^{a,b}, M. Homaei^a

^a Mechanical Engineering Department, Urmia University, Urmia, Iran

^b Institute of Engineering and Technology, South Ural State University, Chelyabinsk, Russian Federation

PAPER INFO

Paper history:

Received 21 October 2019

Received in revised form 03 November 2019

Accepted 08 November 2019

Keywords:

Ultrasound

Micro-speaker

MEMS

Dielectric Elastomers

Bessel Panel

Focused Pressure Pattern

ABSTRACT

Ultrasound wave is a kind of waves with the frequency higher than the human audible frequency. Although ultrasound was first used for military identification purposes, it has been used for decades for various other applications, especially medical applications. Medical applications of ultrasound include diagnostic and therapeutic applications, such as for the treatment of cancer. In this paper, for the first time, electrostatically-actuated micro-speakers made of a dielectric elastomer (DE) have been used to generate and focus the ultrasonic waves using Micro-Electro-Mechanical Systems (MEMS) technology. The results have shown that a single micro-speaker could not generate an efficient focused wave, so an array of the micro-speakers has been considered. The layout of the micro-speakers is a square array of Bessel Panel. It has been shown that by adopting a suitable excitation frequency as well as number of the elements in the Bessel's panel, the DE-based capacitive micro-structures can focus the generated sound wave in a pre-determined area.

doi: 10.5829/ije.2020.33.02b.17

NOMENCLATURE

σ	Maxwell stress	J_1	First order Bessel function
σ_0	Initial pre-stress	[M]	Mass matrix
ε	Relative dielectric permittivity of the elastomer	[B]	Damping matrix
ε_0	Vacuum permittivity	[K]	Stiffness matrix
D	Bending rigidity of the micro-plate	P_p	Acoustic pressure
ν	Poisson's ratio	ρ_0	Air density
∇^4	Biharmonic operator	c_0	Sound velocity in air
∇^2	Laplace operator	k	Wavenumber
T_{str}	Stretching	U_0	Amplitude of the piston's velocity
		ω	excitation frequency

1. INTRODUCTION

There are three types of acoustic waves according to their frequency: A) waves of less than 20Hz is called "subsonic", B) human audible sounds have a frequency of about 20 to 20,000Hz, and C) "Ultrasound" is a sound wave whose frequency exceeds 20,000Hz. In 1876,

Francis Galton first discovered the existence of ultrasound. The initial investigation of ultrasound has been in biologic systems and its biologic effects [1]. Ultrasound is becoming a key and useful instrument in diagnostic and therapeutic tools in current clinical practice. Research on the using of the ultrasound and its medical applications are of great importance today, due

*Corresponding Author Email: m.fathalilou@urmia.ac.ir
(M. Fathalilou)

to the fact that the ultrasound on human tissues does not have the effects of X-ray degradation. In medicine, for example, ultrasound is used to monitor the growth of the fetus in the mother's body and ensure its health. Ultrasound is also used to look for tumors and other abnormal factors in the abdominal cavity, to clean medical and dental devices, to cut body tissues and to examine the heart, also called "Echo Doppler" [2]. It can be said that focusing the ultrasound wave is similar to use of a magnifying glass in sunlight focusing. As a result of this focusing, the temperature rises rapidly at a centralized point (focal zone) of tissue. This is done in such a way that causes the least damage to the surrounding tissues. These waves, by producing acoustic cavities, kill and kill the cancer cells, and increase the temperature above the threshold, leading to the death of tumor cells. In this way, Fry et al. [3] have applied HIFU (High Intensity Focused Ultrasound; ultrasound waves that have power more than $5 \text{ Watt} / m^2$) on the human brain to create discrete lesions to treat hyperkinetic disorders such as Parkinson's disease.

HIFU is a modern and noninvasive therapeutic that treats various of benign and malignant cancers through focusing ultrasound energy to a target tumors tissue such as solid tumors, including prostatic cancer, uterine-fibroids, hepatic tumors, renal tumors, breast cancers, and pancreatic cancers [4]. HIFU has relatively high energy, and in a very small piece of a body can pass through it and be concentrated completely without damaging the tissue [5]. Generated energy of HIFU transducers is focused either mechanically (spherically curved or using a focusing lens) or electronically by phasing an array of transducers [6].

Effects of the HIFU include both thermal and mechanical phenomena in tissue. Thermal effects result from heat generation at the focal zone that it could be caused through the absorption of acoustic energy in the tissue. The absorption of ultrasound energy in the focal zone (in tissue) can raise the temperature rapidly up to 100°C . However, these rapid changes have not a serious effect on intervening tissue between the transducer and the focal zone because the intensities are sufficiently lower outside the focal region. Observations have indicated that if the temperature in the focal zone is raised to 100°C then boiling phenomenon occurs at the focal zone in tissue and coagulative necrosis occurs immediately [7]. Also, HIFU produces mechanical bio-effects in tissue that include acoustic cavitation, radiation force, shear stress and acoustic streaming/micro-streaming. The most significant mechanical phenomenon of the HIFU is acoustic cavitation that occurs when a gas-filled bubble interacts with an ultrasound field [8]. The focal zone characteristics of most clinically available transducers are similar in size to a grain of rice, typically 2-3 mm in diameter and 8-10 mm in length [4]. In addition, it can be applied to perform medical imaging

(diagnostic ultrasound). Diagnostic ultrasound transducer often produces acoustic energy of about $100 \text{ mWatt} / cm^2$, whereas a HIFU transducer can deliver intensities at the focal zone that is over $10 \text{ kWatt} / cm^2$ [9].

Wiktor Staszewski et al. [10] have presented the results of a simulation of the acoustic field distribution in sectors of a 1024-element ring array for the diagnosis of female breast tissue with the use of ultrasonic tomography. Opieliński et al. [11] prototyped a specialist ultrasonic ring array composed of many elementary piezo-ceramic transducers with a rectangular surface, evenly distributed on the inner side of the ring that surrounds the diagnosed breast submerged in water. The ultrasonic tomography scans the whole breast using ultrasonic waves with a frequency of approx. 2 MHz from multiple angles and on many levels. It then processed the data and reconstructs images of individual coronal cross-sections in layers measuring a few millimeters. It has previously been observed that piezoelectric crystals, ceramics and piezo-composite materials have exercised control over the ultrasonic transducer technology. Recent evidence suggests in acoustic applications; capacitors are discovered to be a suitable alternative to piezoelectric materials. Small size and low power consumption are among the most requested characteristics for the acoustic transducers, make the MEMS technology one of the best candidates for their fabrication [12].

The rapid growth of MEMS technology in the field of electrostatically stimulated micro-speakers has made the need for smart materials for these products ever greater [13]. A key aspect of polymer-based audio-range MEMS transducers is that they can be produced inexpensively with batch fabrication to form arrays suitable for macro applications [14]. Two decades ago, new polymers emerged that exhibited significant deformation or size against electrical stimulation. Initially, these materials, i.e. electrically active polymers (EAP), were capable of producing only relatively small strains [15]. But since the early 1990s, a series of new EAP materials have been developed that can produce large strains, resulting in a major change in the capabilities and potentials of these materials. One of the most widely used EAPs is the dielectric elastomer. DEs are elastomers with low elastic modulus and high dielectric fracture toughness [16]. The actuators which are based on a dielectric elastomer (DE) consist of a thin rubber layer, the main surfaces of which are covered by strainable electrodes. By applying an electric field between the electrodes, the electrostatic attraction between the asynchronous charges on the opposite electrodes causes a compressive stress in the thickness direction. The composition of these stresses is expressed as a pure stress in the thickness direction, namely Maxwell stress [17]. Due to its simple mechanism and structure, very large strains (up to 300%)

and good frequency response (1kHz) and good efficiency (60-90%) make the use of DEs very useful in the fabrication of actuators [18].

The main aim of this paper is to investigate the capability of the DE-based micro-speakers for generating the focused ultrasound waves with suitable pressure level. Therefore, for the first time DE-based capacitive micro-speakers have been used to generate and focus the ultrasound wave. The micro-speakers are aligned in a Bessel Panel array. Bessel Panel is a square array of similar micro-speakers in which the elements are spaced together [19]. In this case, the Bessel Panel can be considered as an array with a virtual radius of the length of a row (which is the sum of the radii of the elements in a row and their distance from each other). The effect of the excitation frequency and the number of the elements of the array on the pressure pattern generated by the micro-speakers have also been studied for medical purposes. The results show that the DE-based capacitive micro-speakers can satisfy the need for focusing the ultrasound wave in a predetermined area, which can be used in related applications such as medical applications.

2. MODEL DEFINITION

Figure shows a schematic view of the proposed structure of the micro-speaker. As shown, a capacitive structure is used as a micro-speaker consisting of two circular micro-plates. The bottom micro-plate is fixed and the upper one, made of DE, is suspended on it. Upon applying the voltage between the two micro-plates, the upper micro-plate begins to vibrate. Also, the dielectric voltage is applied between the two electrodes of the upper micro-plate which plays the role of reducing the stiffness of the system. The movable plate is considered with the radius R , uniform thickness h , density ρ , and Young's modulus E . The initial gap between the two plates is g_0 . This MEMS structure in fact is a direct radiator that moves the air molecules directly by its vibrations. As aforementioned, the upper movable plate is a DE having a sandwiched structure consisting of two compliant electrodes at the top and bottom surfaces (Figure).

Due to the confinement of the DE micro-plate boundaries, by applying the electric voltage between the elastomer electrodes, the deformation will produce a compressive stress in the elastomer, known as Maxwell stress, and is defined as follows [18]:

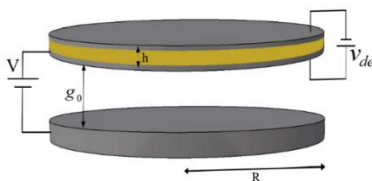


Figure 1. Schematic view of the proposed micro-speaker

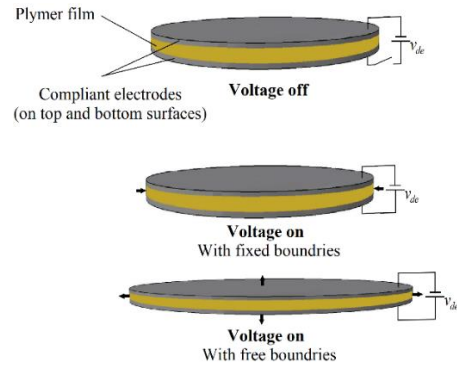


Figure 2. working principle of the DE

$$\sigma = \sigma_0 - \epsilon \epsilon_0 \frac{V_{de}^2}{h^2} \tag{1}$$

where σ_0 is the initial pre-stress, ϵ_0 is the vacuum permittivity, ϵ represents the relative dielectric permittivity of the elastomer and V_{de} is the applied electrical voltage across the plate. The Kirchhoff thin-plate theory is used here for modeling the vibrational behavior of the plate considering the effects of the stretching and the compressive stress caused by the dielectric voltage as follow [20]:

$$D \nabla^4 w + (\sigma h + T_{str}) \nabla^2 w + \rho h \frac{\partial^2 w}{\partial t^2} + c \frac{\partial w}{\partial t} = q \tag{2}$$

where $D = Eh^3/12(1-\nu^2)$ is the bending rigidity of the micro-plate and $T_{str} = \frac{Eh}{2R(1-\nu^2)} \int_0^R \left(\frac{\partial w}{\partial r} \right)^2 dr$ [21]. The damping effects is approximated by an equivalent damping coefficient (viscous damping) c per unit length. ∇^4 and ∇^2 are the biharmonic operator and the Laplace operator in the polar coordinate system, respectively, well-determined as follows:

$$\nabla^4 = \nabla^2(\nabla^2) = \left(\frac{\partial^2}{\partial r^2} + \frac{1}{r} \frac{\partial}{\partial r} + \frac{1}{r^2} \frac{\partial^2}{\partial \theta^2} \right) \left(\frac{\partial^2}{\partial r^2} + \frac{1}{r} \frac{\partial}{\partial r} + \frac{1}{r^2} \frac{\partial^2}{\partial \theta^2} \right) \tag{3}$$

Due to the symmetry of the microplate vibrations, the angular terms are ignored. The electrostatic pressure of the microplate is nonlinear and results from the approximation of the parallel plate under applied voltage as defined below [22]:

$$q(v, w) = \frac{\epsilon_0 V^2(t)}{2(g_0 - w)^2} \tag{4}$$

Moreover, the fully-clamped boundary conditions are defined as $w(R, t) = 0$, $\frac{\partial}{\partial r} w(R, t) = 0$.

3. NUMERICAL SOLUTION

To generalize the equation and facilitate the analysis, we first change the governing equation to dimensionless form by defining the dimensionless parameters as:

$$w = \frac{W}{g_0}, \quad r = \frac{r}{R}, \quad \hat{t} = \frac{t}{t^*}, \quad t^* = R^2 \sqrt{\frac{\rho h}{D}}, \quad w = wt^* \quad (5)$$

By replacement of these dimensionless parameters in the governing equation (Equation (1)), the dimensionless equation is obtained as follows:

$$\begin{aligned} \nabla^4 w + \beta \nabla^2 w + \frac{\partial^3 w}{\partial t^2} + C \frac{\partial w}{\partial t} &= \frac{\alpha V^2}{(1-w)^2} \\ \beta &= \frac{R^2}{D} \sigma h + \frac{g_0^2 R}{D} T_{str}, \quad C = cR^2 \sqrt{\frac{1}{\rho h D}}, \\ \alpha &= \frac{\epsilon_0 R^4}{2g_0^3 D} \end{aligned} \quad (6)$$

The overall displacement of the microplate is assumed to be divided into two parts due to the applied DC and AC voltage. First is the static displacement caused by the applied DC voltage, and the microplate reaches a static equilibrium position (this is due to the control of the resonance frequency), and the dynamic motion caused by the AC voltage, which is applied then, and the microplate starts to vibrate around the static equilibrium. The AC voltage is considered to be much smaller than the DC voltage to reduce the order of the geometrical nonlinear behavior. So, the total displacement can be written as follow:

$$w(\hat{r}, \hat{t}) = \hat{w}_s(\hat{r}) + \hat{w}_d(\hat{r}, \hat{t}) \quad (7)$$

By linearization of the nonlinear electrostatic and stretching terms about equilibrium position, we have the following linear equation:

$$\begin{aligned} \nabla^4 (\hat{w}_s + \hat{w}_d) + \beta \nabla^2 (\hat{w}_s + \hat{w}_d) + \frac{\partial^3 \hat{w}_d}{\partial \hat{t}^2} + C \frac{\partial \hat{w}_d}{\partial \hat{t}} &= \\ \frac{\alpha V_{DC}^2}{(1-\hat{w}_s)^2} + \frac{2\alpha V_{DC} V_{AC}}{(1-\hat{w}_s)^2} + \frac{2\alpha V_{DC}^2}{(1-\hat{w}_s)^3} \hat{w}_d \end{aligned} \quad (8)$$

3. 1. Static Solution

Eliminating the time-dependent terms from the Equation (6), the static equation is obtained as follow:

$$\nabla^4 \hat{w}_s + \beta \nabla^2 \hat{w}_s = \frac{\alpha V_{DC}^2}{(1-\hat{w}_s)^2} \quad (9)$$

This equation is nonlinear that has no analytical solution, so it should be solved numerically. To solve it, we first linearize the equation using Step by Step Linearization Method (SSLM) [23] and then the Galerkin method is used, which is finally results in the following equation [23]:

$$\sum_{j=1}^n K_{ij} a_j = F_i \quad \text{and} \quad K_{ij} = k_{ij}^{mech} - k_{ij}^{elec} \quad (10)$$

where

$$\begin{aligned} k_{ij}^{mech} &= \int_0^1 \phi_i(\hat{r}) \left(\phi_j^{(IV)}(\hat{r}) + \frac{2}{\hat{r}} \phi_j''(\hat{r}) - \frac{1}{\hat{r}^2} \phi_j'(\hat{r}) + \frac{1}{\hat{r}^3} \phi_j'(\hat{r}) + \beta \phi_j'(\hat{r}) + \beta \frac{1}{\hat{r}} \phi_j'(\hat{r}) \right) dr \\ k_{ij}^{elec} &= \frac{2\alpha V_{DC}^2}{(1-\hat{w}_s^k)^3} \int_0^1 \phi_j(\hat{r}) \phi_i(\hat{r}) dr, \quad F_i = \frac{2\alpha V_{DC} \delta V}{(1-\hat{w}_s^k)^2} \int_0^1 \phi_i(\hat{r}) dr \end{aligned} \quad (11)$$

3. 2. Dynamic Solution

By subtracting the static Equation () from the governing linearized Equation (), the equation of motion is obtained as follow:

$$\begin{aligned} \nabla^4 \hat{w}_d + \beta \nabla^2 \hat{w}_d + \frac{\partial^3 \hat{w}_d}{\partial \hat{t}^2} + C \frac{\partial \hat{w}_d}{\partial \hat{t}} - \\ \frac{2\alpha V_{DC}^2}{(1-\hat{w}_s)^3} \hat{w}_d = \frac{2\alpha V_{DC} V_0 \sin(\hat{\omega} \hat{t})}{(1-\hat{w}_s)^2} \end{aligned} \quad (12)$$

To solve this, first Mode Summation method is used and then by using the Galerkin method the following equation is obtained:

$$[\mathbf{M}] \ddot{\mathbf{q}}(t) + [\mathbf{B}] \dot{\mathbf{q}}(t) + [\mathbf{K}] \mathbf{q}(t) = \mathbf{F} \sin(\alpha t) \quad (13)$$

This equation is a set of coupled differential equations that can be solved using the Runge-Kutta method [23], where:

$$\begin{aligned} M_{ij} &= \int_0^1 \phi_i(\hat{r}) \phi_j(\hat{r}) dr, \quad B_{ij} = \beta \int_0^1 \phi_i(\hat{r}) \phi_j(\hat{r}) dr, \\ k_{ij}^{mech} &= \int_0^1 \phi_i(\hat{r}) \left(\phi_j^{(IV)}(\hat{r}) + \frac{2}{\hat{r}} \phi_j''(\hat{r}) - \frac{1}{\hat{r}^2} \phi_j'(\hat{r}) + \frac{1}{\hat{r}^3} \phi_j'(\hat{r}) + \beta \phi_j'(\hat{r}) + \beta \frac{1}{\hat{r}} \phi_j'(\hat{r}) \right) dr, \\ k_{ij}^{elec} &= \frac{2\alpha V_{DC}^2}{(1-\hat{w}_s)^3} \int_0^1 \phi_j(\hat{r}) \phi_i(\hat{r}) dr, \\ F_i &= \frac{\alpha V_{DC}^2}{\left(1 - \sum_{\tau=1}^N q(t) \phi_\tau(r)\right)^2} \int_0^1 \phi_j(\hat{r}) dr \end{aligned} \quad (1)$$

4. SOUND PRESSURE CALCULATION

As aforementioned, to enhance the generated sound pressure level (SPL) and reach the desired focused waves we need to have an array of the micro-speakers that can be arranged in a Bessel panel array [24]. The schematic of the used Bessel panel is shown in Figure 3:

The methods and equations described in this section will be used to predict the performance of the Bessel panel array. In this paper, the elastic circular micro-plate is considered as a medium-radius with average radius, R which is mounted inside an infinite baffle (half space).

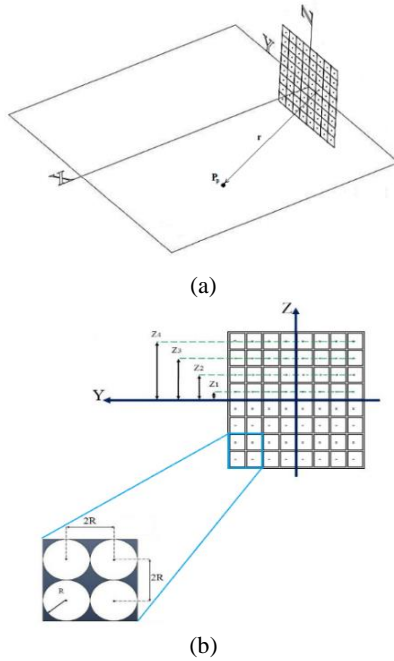


Figure 3. a) Schematic of the Bessel panel array and one of the points of working plane with distance r from one of sources, b) Front view with inter element spacing $2R$

The radiating surface of the circular acoustic source moves uniformly with speed $U_0 \exp(j\omega t)$ normal to the baffle. This radiator is also considered as a piston that emits ultrasound only in its forward direction [24]. In this study the effect of the mechanical impedance of the ultrasonic source as well as the impedance of the diffusion medium are not considered.

For the mathematical formulation of the pressure generated from the sources, due to the small size of the micro-speakers, the integral formulation on the micro-speaker elements is neglected and each source in the Bessel panel array is considered as a point source. Under these assumptions, the pressure generated from each source at the desired point p is given as follows [24].

$$P_p(r, \theta) = \frac{j \rho_0 c_0 k U_0 R^2}{2r} \exp(\alpha t - kr) \left[\frac{2J_1(kR \sin \theta)}{kR \sin \theta} \right] \quad (2)$$

where P_p is the acoustic pressure, R is the piston radius, ρ_0 is the density of air, c_0 is the sound velocity in air, k is the wavenumber, U_0 is the amplitude of the piston's velocity, and ω is the excitation frequency. The obtained pressure relation consists of two parts; the first part includes components such as velocity amplitude of the piston, piston size, and distance from the source. The second part is the piston directivity function that is derived from the first type of Bessel function, $J_1(kR \sin \theta)$.

In the Bessel panel array, if the number of elements is large enough, each row of omnidirectional sources (a source which its radiations emits in all directions) can be defined as a discrete array such as Figure 4. By defining a discrete array, the second part of the pressure calculation formula will be changed to the following formula [25].

$$D(\theta) = \left| \frac{\sin \left(N \frac{\pi d}{\lambda} (\sin \theta - \sin(\theta_s)) \right)}{N \sin \left(\frac{\pi d}{\lambda} (\sin \theta - \sin(\theta_s)) \right)} \right| \quad (16)$$

where N is the number of sources, θ_s the derived angle, and d the distance between the elements. θ_s is obtained from the height of discrete array of worksheets and the longitudinal distance of the focus point as Figure 5.

In order to focus the ultrasound in addition to control the radiation pattern, we first need to have a rectified wave propagation pattern. This prevents the transmission of ultrasound to other non-target areas and also increases the concentration power. For this purpose, two key parameters of the wavelength and the virtual radius of the Bessel panel are effective i.e. (R'/λ) . As the excitation frequency increases, the wavelength decreases and will improve to a one-way pattern. Increasing the virtual radius will also help to have a single pattern [24] so that the radius of the elements, the distance between the elements or their number can be changed.

5. RESULT AND DISCUSSION

TABLE 1 shows the physical and geometrical properties of the system considered in this paper [16]. In the first step, it is necessary to calculate the pull-in voltage of the microplate as the audio source, because we should ensure that the system under the applied voltages would not experience the pull-in instability.

It should be noted that the dielectric voltage of 30V is applied to the dielectric elastomer for softening the plate

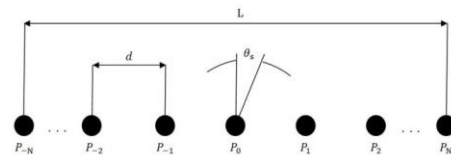


Figure 4. A discrete array

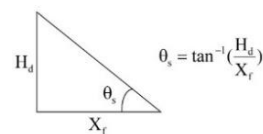


Figure 5. Illustration of the θ_s

TABLE 1. Properties of the microplate [16]

Radius	500 μ m
Thickness	2 μ m
Initial gap	4 μ m
Young's modulus	3GPa
Density	1.226 kg/m ³
Poisson's ratio	0.5
Dielectric elastomer pre-strain	1kPa
Dielectric elastomer permittivity	16
Dielectric elastomer Voltage	30 V

and thereby increase the efficiency of the ultrasonic source. Variations of the center gap of the capacitor with the applied DC voltage is shown in Figure 6 up to the pull-in voltage. According to Figure 6, the pull-in occurs at 2.71V.

Figure 7 shows the sound pressure pattern generated by a single DE-based micro-speaker with the properties of Table 1. The excitation frequency is considered to be 5 MHz. As gained from this figure, a single micro-speaker could not generate a focused pattern for the sound pressure. Also the magnitude of the generated pressure is too low. So, we should consider an array of micro-speakers, namely Bessel panel array to produce the higher levels of sound pressures, of course with focused pattern.

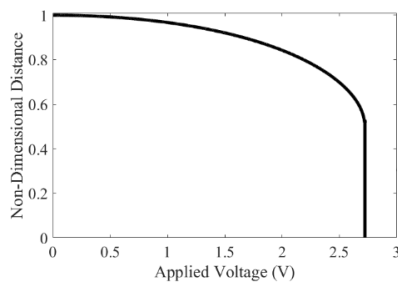


Figure 6. Nondimensional gap versus applied DC voltage

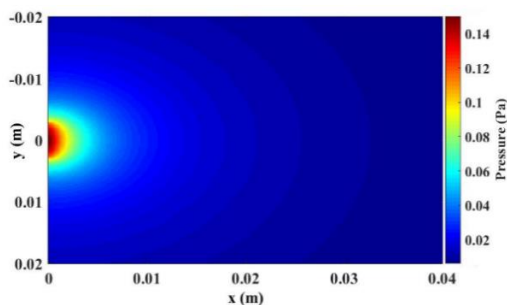
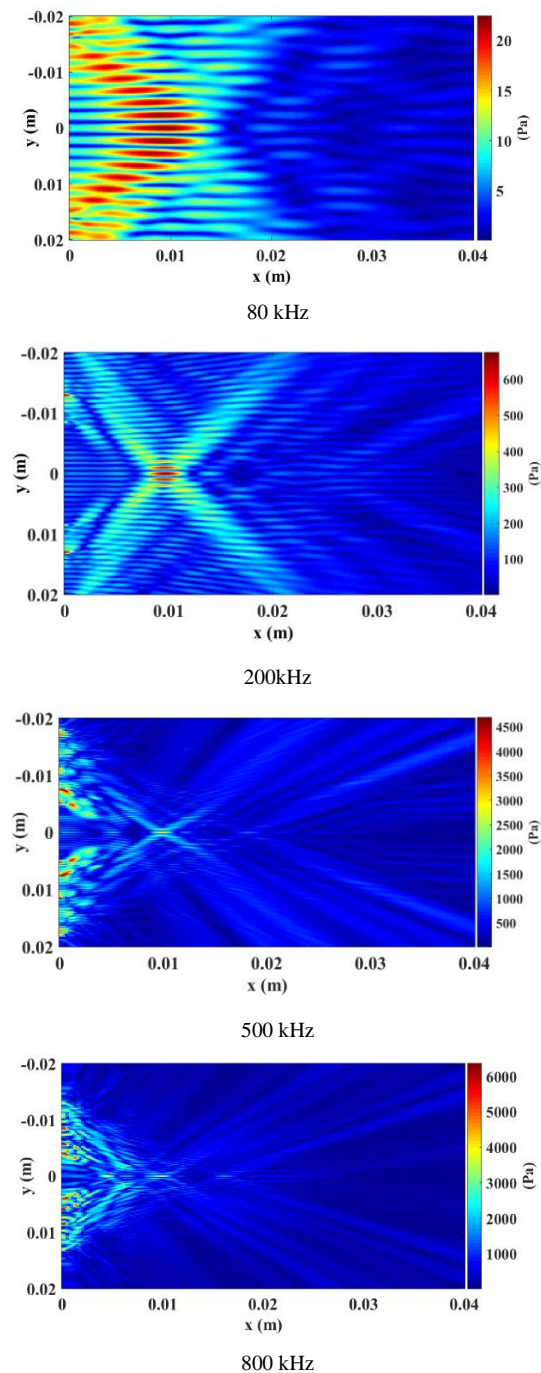


Figure 7. Sound wave propagation pattern for a single micro-speaker

First, we consider an array of 100 micro-speakers which are in a Bessel panel array at a distance of 2*R and show the wave propagation pattern with different excitation frequencies as Figure 8.

The pressures at the focal zone for all cases are given in Table 2.

As shown in Figure 8, at a fixed virtual radius (which, as stated earlier, the summation of the radii of the elements in a row of Bessel panel array and the



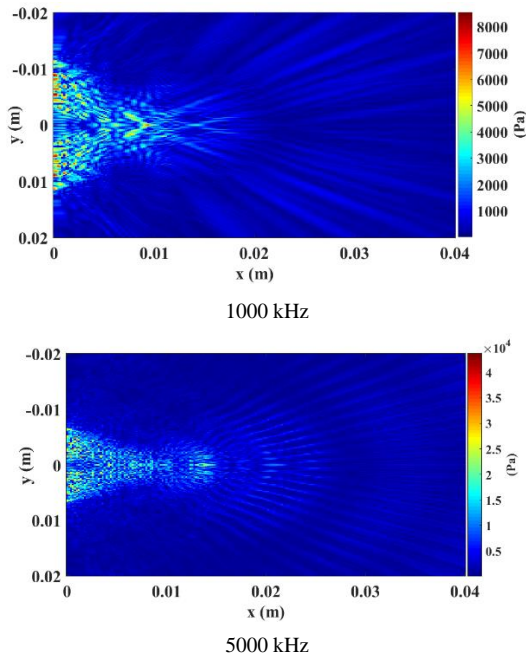


Figure 8. Effect of excitation frequency changes on the pressure concentration pattern

TABLE 2. Pressure at the 1cm from the Bessel panel array with different excitation frequencies

f_{exc} (kHz)	Pressure (Pa)
80	22.22
200	655.6
500	2989
800	3216
1000	3976
5000	1.535e+04

distance between them forms the virtual radius), increasing the frequency as a result, decreasing the wavelength ($\lambda = c/f$) improves the directivity pattern and cause increases in the centralization effect. Moreover, as shown in Table 2, by increasing the excitation frequency the pressure of the sound in the focal zone increases.

Figure 9 illustrates the effects of the number of elements on the concentrated pressure pattern. It should be noted that the excitation frequency is considered to be 800 kHz here.

Figure 9 shows that as the number of the elements increases, the virtual radius increases and at a constant frequency, this results in an increase in the R'/λ ratio, so we have a more appropriate focused pattern. Also, Table

3 confirms that by increasing the number of elements, we have the higher sound pressure in the focal zone.

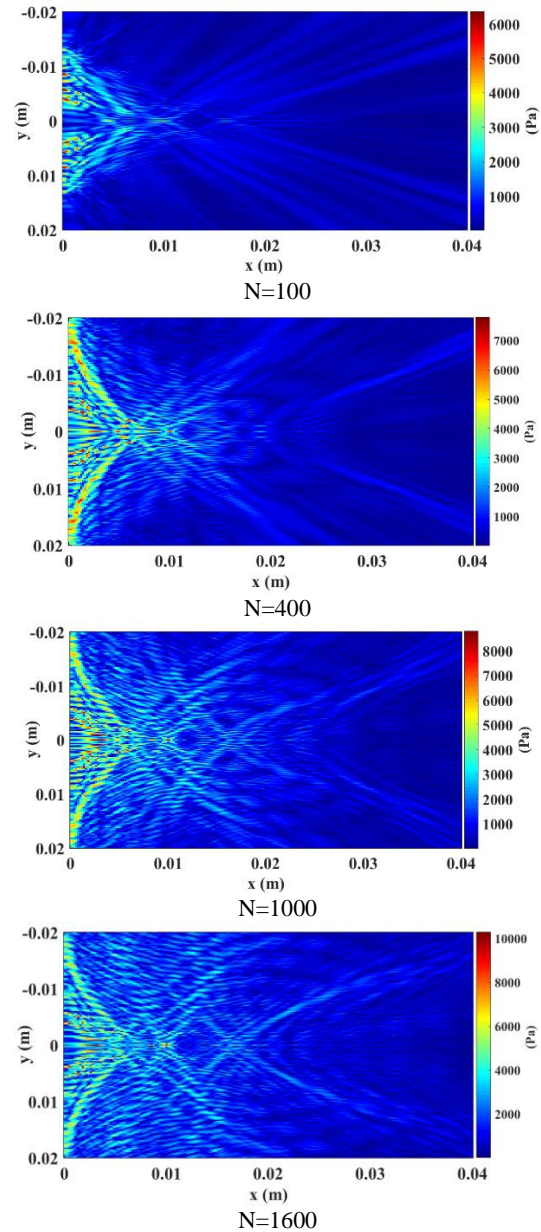


Figure 9. Effects of the number of the elements on the concentration pattern

TABLE 3. Pressure at the 1cm from the Bessel panel array with different number of elements

Elements Number	Pressure (Pa)
100	3216
400	6426
1000	8410
1600	9822

6. CONCLUSION

This paper investigated the capability of the DE-based capacitive micro-speakers to generate the ultrasonic waves. It also focused on the capability to concentrate the pressure pattern generated by these micro-speakers arrayed in a Bessel panel. The results showed that a single capacitive micro-structure cannot generate an enough sound pressure with the centralized pattern. So, we tried to consider an array of micro-speakers aligned in the Bessel panel. It was shown that, as the excitation frequency of the speakers of the Bessel panel increased, the magnitude of the sound wave pressure and its centralized pattern were improved. The increase in the number of elements also resulted in the improvement of the concentration and magnitude of the pressure as well. Generally, this investigation showed that the DE-based capacitive micro-speakers have the ability to be used in the applications which needs focused ultrasound waves such as medical applications. The results can be useful for developing the medical instruments.

7. REFERENCES

- Harvey, E.N., Loomis A.L., "High frequency sound waves of small intensity and their biological effects". *Nature Publishing Group*. Vol. 121, (1928), 622-624.
- Murad, H.Y., "High intensity focused ultrasound (HIFU) in conjunction with thermally triggered chemotherapy as a synergistic treatment of cancer". Tulane University School of Science and Engineering, (2016).
- Fry, W., Fry, F., "Fundamental neurological research and human neurosurgery using intense ultrasound". *IRE Transactions on Medical Electronics*, Vol. 7, (1960), 166-181.
- Jang, H.J., Lee, J.Y., Lee, D.H., Kim, W.H. and Hwang, J.H., "Current and future clinical applications of high-intensity focused ultrasound (HIFU) for pancreatic cancer". *Gut and Liver*, Vol. 4, (2010), S57-S61.
- Minin, O., Minin, I., "Ultrasound Imaging: Medical Applications". BoD—Books on Demand. (2011).
- Opieliński, K., "Application of transmission of ultrasonic waves for characterization and imaging of biological media structures". Printing House of Wrocław University of Science and Technology, Wrocław, (2011).
- Azhari, H., "Basics of biomedical ultrasound for engineers". John Wiley & Sons (2010).
- Escoffre, J.M., Bouakaz, A., "Therapeutic ultrasound". Springer Vol. 880, (2015).
- Allan, P.L., Baxter, G.M. and Weston, M.J. "Clinical Ultrasound". E-Book: Expert Consult: Online and Print. Elsevier Health Sciences Vol 2, (2011).
- Staszewski, W., Gudra, T., and Opieliński, K., "The Acoustic Field Distribution Inside the Ultrasonic Ring Array". *Archives of Acoustics*, Vol. 43, No. 3, (2018). 455–463.
- Opieliński, K.J., Pruchnicki, P., Szymanowski P., "Multimodal ultrasound computer-assisted tomography: An approach to the recognition of breast lesions". *Computerized Medical Imaging and Graphics*, Vol. 65, (2018), 102-114.
- De Pasquale, G., Rufer, L., Basrou, S., and Somà, A., "Modeling and validation of acoustic performances of micro-acoustic sources for hearing applications". *Sensors and Actuators A: Physical*, Vol. 247, (2016), 614-628.
- Varadan, V.K., Vinoy, K.J., Jose, K.A., "Their Applications". Pennsylvania State University, USA, Wiley Online Library, (2003).
- Heydt, R., Kornbluh, R., Eckerle, J., "Sound radiation properties of dielectric elastomer electroactive polymer loudspeakers". *Smart Structures and Materials. Electroactive Polymer Actuators and Devices (EAPAD)*. Vol. 6168, (2006), 1-8.
- Bar-Cohen, Y., "Electroactive polymer (EAP) actuators as artificial muscles: reality, potential, and challenges". SPIE press Bellingham, WA., Vol. 136., (2004).
- Feng, C., Jiang, L. and Lau, W.M., "Dynamic characteristics of a dielectric elastomer-based microbeam resonator with small vibration amplitude". *Journal of Micromechanics and Micro engineering*, Vol. 21, (2011), 095002.
- Sarban, R., Jones, R.W., Mace, B.R. and Rustighi, E., "A tubular dielectric elastomer actuator: Fabrication, characterization and active vibration isolation". *Mechanical Systems and Signal Processing*, Vol. 25, (2011), 2879-2891.
- Carpi, F., Rossi, D., Kornbluh, R. and Pelrine, R.E., "Dielectric elastomers as electromechanical transducers". Fundamentals, materials, devices, models and applications of an emerging electroactive polymer technology, Elsevier. (2011).
- Keele Jr, D., "Effective performance of Bessel arrays". *Journal of the Audio Engineering Society*, Vol. 38, (1990), 723-748.
- Reddy, J.N., "Energy and variational methods in applied mechanics: with an introduction to the finite element method". Wiley New York, (1984).
- Varadan, V.K., Vinoy, K.J. and Jose, K.A., "RF MEMS and their Applications". Pennsylvania State University, USA, (2003).
- Mostafaei, B., Fathalilou, M., and Rezazadeh, G., "A comparative analysis of efficiency and reliability of capacitive micro-switches with initially curved electrodes". *Microsystem Technologies*, (2019), online available.
- Rezazadeh, G., Fathalilou, M., and Shabani, R., "Static and dynamic stabilities of a microbeam actuated by a piezoelectric voltage". *Microsystem Technologies*, Vol. 15, (2009), 1785-1791.
- Kinsler, L.E., Frey A.R., Coppens, A.B., Sanders, J.V., "Fundamentals of acoustics. Fundamentals of Acoustics". 4th Edition, Wiley-VCH, pp. 560. ISBN 0-471-84789-5. (December 1999), 560.
- Kuttruff, H., "Acoustics: an introduction". CRC Press. (2006).

Generating and Focusing the Ultrasound Waves Using Elastomer-based Capacitive Micro-Speakers

M. Soosani^a, M. Fathalilou^a, G. Rezazadeh^{a,b}, M. Homaei^a

^a Mechanical Engineering Department, Urmia University, Urmia, Iran

^b Institute of Engineering and Technology, South Ural State University, Chelyabinsk, Russian Federation

PAPER INFO

چکیده

Paper history:

Received 21 October 2019

Received in revised form 03 November 2019

Accepted 08 November 2019

Keywords:

Ultrasound

Micro-speaker

MEMS

Dielectric Elastomers

Bessel Panel

Focused Pressure Pattern

امواج فراصوتی به امواجی گفته می‌شود که بسامدی بالاتر از شنوایی انسان دارند. اگرچه اولین بار از امواج فراصوتی برای کاربرد شناسایی در حیطه‌ی نظامی استفاده شد، اکنون دهه‌هاست که از این امواج برای کاربردهای مختلف دیگری به‌خصوص کاربردهای پزشکی استفاده می‌شود. کاربرد پزشکی امواج فراصوتی شامل کاربردهای تشخیصی و کاربردهای درمانی (مثلاً برای درمان سرطان) می‌باشد. در این مقاله، برای اولین بار از میکروبلندگوهای با تحریک الکترواستاتیکی ساخته شده از الاستومرهای دی‌الکتریک برای تولید و متمرکزسازی امواج اولتراسوند با استفاده از تکنولوژی MEMS استفاده شده است. نتایج نشان داده‌اند که یک میکروبلندگوی تنها قادر به تولید موج صوتی متمرکز مناسب نیست، بنابراین آرایه‌ای از میکروبلندگوها در نظر گرفته شده است. چیدمان میکروبلندگوها به‌صورت آرایه‌ی مربعی بسل پتل می‌باشد. نشان داده شده است که با اتخاذ مقادیر مناسب برای بسامد تحریک سیستم و نیز تعداد بلندگوهای تعبیه شده در آرایه‌ی بسل، میکروبلندگوهای خازنی ساخته شده از الاستومر می‌توانند امواج صوتی تولید شده را در ناحیه‌ی ازپیش تعیین شده متمرکز سازند.

doi: 10.5829/ije.2020.33.02b.17